



# Measurement of double-polarization asymmetries in the quasi-elastic $^3\text{He}(\vec{e}, e'p)$ process

The Jefferson Lab Hall A Collaboration

M. Mihovilovič<sup>a,b,c</sup>, G. Jin<sup>d</sup>, E. Long<sup>e</sup>, Y.-W. Zhang<sup>f</sup>, K. Allada<sup>g</sup>, B. Anderson<sup>h</sup>, J.R.M. Annand<sup>i</sup>, T. Averett<sup>j</sup>, W. Bertozzi<sup>k</sup>, W. Boeglin<sup>l</sup>, P. Bradshaw<sup>j</sup>, A. Camsonne<sup>g</sup>, M. Canan<sup>m</sup>, G.D. Cates<sup>d</sup>, C. Chen<sup>n</sup>, J.P. Chen<sup>g</sup>, E. Chudakov<sup>g</sup>, R. De Leo<sup>o</sup>, X. Deng<sup>d</sup>, A. Deltuva<sup>p</sup>, A. Deur<sup>g</sup>, C. Dutta<sup>q</sup>, L. El Fassi<sup>f</sup>, D. Flay<sup>r</sup>, S. Frullani<sup>s</sup>, F. Garibaldi<sup>s</sup>, H. Gao<sup>t</sup>, S. Gilad<sup>k</sup>, R. Gilman<sup>f</sup>, O. Glamazdin<sup>u</sup>, J. Golak<sup>v</sup>, S. Golge<sup>m</sup>, J. Gomez<sup>g</sup>, O. Hansen<sup>g</sup>, D.W. Higinbotham<sup>g</sup>, T. Holmstrom<sup>w</sup>, J. Huang<sup>k</sup>, H. Ibrahim<sup>x</sup>, C.W. de Jager<sup>g,†</sup>, E. Jensen<sup>y</sup>, X. Jiang<sup>z</sup>, M. Jones<sup>g</sup>, H. Kamada<sup>aa</sup>, H. Kang<sup>ab</sup>, J. Katich<sup>j</sup>, H.P. Khanal<sup>l</sup>, A. Kievsky<sup>ac</sup>, P. King<sup>ad</sup>, W. Korsch<sup>q</sup>, J. LeRose<sup>g</sup>, R. Lindgren<sup>d</sup>, H.-J. Lu<sup>ae</sup>, W. Luo<sup>af</sup>, L.E. Marcucci<sup>ac</sup>, P. Markowitz<sup>l</sup>, M. Mezziane<sup>j</sup>, R. Michaels<sup>g</sup>, B. Moffit<sup>g</sup>, P. Monaghan<sup>n</sup>, N. Muangma<sup>k</sup>, S. Nanda<sup>g</sup>, B.E. Norum<sup>d</sup>, K. Pan<sup>k</sup>, D.S. Parno<sup>ag</sup>, E. Piasetzky<sup>ah</sup>, M. Posik<sup>r</sup>, V. Punjabi<sup>ai</sup>, A.J.R. Puckett<sup>aj</sup>, X. Qian<sup>t</sup>, Y. Qiang<sup>g</sup>, X. Qui<sup>af</sup>, S. Riordan<sup>d</sup>, A. Saha<sup>g,†</sup>, P.U. Sauer<sup>ak</sup>, B. Sawatzky<sup>g</sup>, R. Schiavilla<sup>g,m</sup>, B. Schoenrock<sup>al</sup>, M. Shabestari<sup>d</sup>, A. Shahinyan<sup>am</sup>, S. Širca<sup>a,b,\*</sup>, R. Skibiński<sup>v</sup>, J. St. John<sup>w</sup>, R. Subedi<sup>an</sup>, V. Sulkosky<sup>k</sup>, W. Tireman<sup>al</sup>, W.A. Tobias<sup>d</sup>, K. Topolnicki<sup>v</sup>, G.M. Urciuoli<sup>s</sup>, M. Viviani<sup>ac</sup>, D. Wang<sup>d</sup>, K. Wang<sup>d</sup>, Y. Wang<sup>ao</sup>, J. Watson<sup>g</sup>, B. Wojtsekhowski<sup>g</sup>, H. Witała<sup>v</sup>, Z. Ye<sup>n</sup>, X. Zhan<sup>k</sup>, Y. Zhang<sup>af</sup>, X. Zheng<sup>d</sup>, B. Zhao<sup>j</sup>, L. Zhu<sup>n</sup>

<sup>a</sup> Faculty of Mathematics and Physics, University of Ljubljana, SI-1000 Ljubljana, Slovenia

<sup>b</sup> Jožef Stefan Institute, SI-1000 Ljubljana, Slovenia

<sup>c</sup> Institut für Kernphysik, Johannes Gutenberg-Universität Mainz, DE-55128 Mainz, Germany

<sup>d</sup> University of Virginia, Charlottesville, VA 22908, USA

<sup>e</sup> University of New Hampshire, Durham, NH 03824, USA

<sup>f</sup> Rutgers University, New Brunswick, NJ 08901, USA

<sup>g</sup> Thomas Jefferson National Accelerator Facility, Newport News, VA 23606, USA

<sup>h</sup> Kent State University, Kent, OH 44242, USA

<sup>i</sup> Glasgow University, Glasgow G12 8QQ, Scotland, United Kingdom

<sup>j</sup> The College of William and Mary, Williamsburg, VA 23187, USA

<sup>k</sup> Massachusetts Institute of Technology, Cambridge, MA 02139, USA

<sup>l</sup> Florida International University, Miami, FL 33181, USA

<sup>m</sup> Old Dominion University, Norfolk, VA 23529, USA

<sup>n</sup> Hampton University, Hampton, VA 23669, USA

<sup>o</sup> Università degli studi di Bari Aldo Moro, I-70121 Bari, Italy

<sup>p</sup> Institute for Theoretical Physics and Astronomy, Vilnius University, LT-01108 Vilnius, Lithuania

<sup>q</sup> University of Kentucky, Lexington, KY 40506, USA

<sup>r</sup> Temple University, Philadelphia, PA 19122, USA

<sup>s</sup> Istituto Nazionale Di Fisica Nucleare, INFN/Sanita, Roma, Italy

<sup>t</sup> Duke University, Durham, NC 27708, USA

<sup>u</sup> Kharkov Institute of Physics and Technology, Kharkov 61108, Ukraine

<sup>v</sup> M. Smoluchowski Institute of Physics, Jagiellonian University, PL-30348 Kraków, Poland

<sup>w</sup> Longwood College, Farmville, VA 23909, USA

<sup>x</sup> Cairo University, Cairo, Giza 12613, Egypt

\* Corresponding author at: Faculty of Mathematics and Physics, University of Ljubljana, SI-1000 Ljubljana, Slovenia.

E-mail address: [simon.sirca@fmf.uni-lj.si](mailto:simon.sirca@fmf.uni-lj.si) (S. Širca).

† Deceased.

<sup>y</sup> Christopher Newport University, Newport News, VA 23606, USA

<sup>z</sup> Los Alamos National Laboratory, Los Alamos, NM 87545, USA

<sup>aa</sup> Department of Physics, Faculty of Engineering, Kyushu Institute of Technology, Kitakyushu 804-8550, Japan

<sup>ab</sup> Seoul National University, Seoul, Republic of Korea

<sup>ac</sup> INFN-Pisa, I-56127 Pisa, Italy

<sup>ad</sup> Ohio University, Athens, OH 45701, USA

<sup>ae</sup> Huangshan University, People's Republic of China

<sup>af</sup> Lanzhou University, Lanzhou, Gansu, 730000, People's Republic of China

<sup>ag</sup> Carnegie Mellon University, Pittsburgh, PA 15213, USA

<sup>ah</sup> Tel Aviv University, Tel Aviv 69978, Israel

<sup>ai</sup> Norfolk State University, Norfolk, VA 23504, USA

<sup>aj</sup> University of Connecticut, Storrs, CT 06269, USA

<sup>ak</sup> Institute for Theoretical Physics, University of Hannover, D-30167 Hannover, Germany

<sup>al</sup> Northern Michigan University, Marquette, MI 49855, USA

<sup>am</sup> Yerevan Physics Institute, Yerevan, Armenia

<sup>an</sup> George Washington University, Washington, DC 20052, USA

<sup>ao</sup> University of Illinois at Urbana-Champaign, Urbana, IL 61801, USA

## ARTICLE INFO

### Article history:

Received 6 July 2018

Received in revised form 22 October 2018

Accepted 31 October 2018

Available online 5 November 2018

Editor: V. Metag

### Keywords:

Double-polarization asymmetry

Helium-3 nucleus

Proton knock-out

## ABSTRACT

We report on a precise measurement of double-polarization asymmetries in electron-induced breakup of  $^3\text{He}$  proceeding to pd and ppn final states, performed in quasi-elastic kinematics at  $Q^2 = 0.25 (\text{GeV}/c)^2$  for missing momenta up to 250 MeV/c. These observables represent highly sensitive tools to investigate the electromagnetic and spin structure of  $^3\text{He}$  and the relative importance of two- and three-body effects involved in the breakup reaction dynamics. The measured asymmetries cannot be satisfactorily reproduced by state-of-the-art calculations of  $^3\text{He}$  unless their three-body segment is adjusted, indicating that the spin-dependent part of the nuclear interaction governing the three-body breakup process is much smaller than previously thought.

© 2018 The Author. Published by Elsevier B.V. This is an open access article under the CC BY license (<http://creativecommons.org/licenses/by/4.0/>). Funded by SCOAP<sup>3</sup>.

The  $^3\text{He}$  nucleus represents the key challenge of nuclear physics due to its potential to reveal the basic features of nuclear structure and dynamics in general. In particular, this paradigmatic three-body system offers a unique opportunity to study the interplay of two-nucleon and three-nucleon interactions, an effort at the forefront of nuclear physics research [1–4]. Modern theoretical descriptions of the structure and dynamics of  $^3\text{He}$  require, first of all, a detailed understanding of the nuclear Hamiltonian (including the three-nucleon force), which generates the consistent nuclear ground and scattering states, while accounting for final-state interactions (FSI). The reaction mechanism comprises also the electromagnetic current operator, which takes into account meson-exchange currents (MEC). Experiments on  $^3\text{He}$ , particularly those involving polarization degrees of freedom, provide essential input to theories which need to be perpetually improved to yield better understanding of the underlying physics and to match the current increase in experimental precision. The quality of theoretical models is crucial to all  $^3\text{He}$ -based experiments seeking to extract neutron information by utilizing  $^3\text{He}$  as an effective neutron target, an approximation relying on a sufficient understanding of the proton and neutron polarization within polarized  $^3\text{He}$ .

The  $^3\text{He}$  nucleus is best studied by electron-induced knockout of protons, deuterons and neutrons, where the sensitivity to various aspects of the process can be greatly enhanced by the use of polarized beam and target [2]. The focus of this paper is on the two-body (2bbu) and three-body (3bbu) breakup channels with proton detection in the final state,  $^3\text{He}(\vec{e}, e'p)d$  and  $^3\text{He}(\vec{e}, e'p)pn$ , which were investigated concurrently with the already published  $^3\text{He}(\vec{e}, e'd)$  data [5].

In a  $^3\text{He}(\vec{e}, e'p)$  reaction the virtual photon emitted by the incoming electron transfers the energy  $\omega$  and momentum  $\mathbf{q}$  to the  $^3\text{He}$  nucleus. The process observables are then analyzed in terms of missing momentum, defined as the difference between the momentum transfer and the detected proton momentum,  $p_m = |\mathbf{q} - \mathbf{p}_p|$ , thus  $p_m$  corresponds to the momentum of the recoiled

deuteron in 2bbu and the total momentum of the residual pn system in 3bbu.

The unpolarized  $^3\text{He}(e, e'p)$  process at low energies has been studied at MAMI, both on the quasi-elastic peak [6] and below it [7]. The bulk of our present high-energy information comes from experiments in quasi-elastic kinematics at Jefferson Lab [8–10], resulting in reaction cross-sections at high  $p_m$  and yielding important insight into nucleon momentum distributions, isospin structure of the transition currents, FSI, and MEC [11–15]. However, just as in the  $(e, e'd)$  case, experiments that exploit polarization offer much greater sensitivity to the fine details of these ingredients. Such measurements have been extremely scarce. A single asymmetry data point with high uncertainty exists from NIKHEF [16,17]. In addition, we have a precise measurement of both transverse and longitudinal asymmetries separately for the 2bbu and 3bbu channels in quasi-elastic kinematics [18,19], but the measurement was restricted to (and summed over) relatively low  $p_m$ .

Early theoretical studies [20–22] have shown strong sensitivities of double-polarization asymmetries in  $^3\text{He}$  breakup to the isospin structure of the electromagnetic current, to the sub-leading components of the  $^3\text{He}$  ground-state wave-function, as well as to the tensor component of the nucleon–nucleon interaction. However, while in the deuteron channel these would predominantly manifest themselves at low  $p_m$ , the 2bbu and 3bbu proton channels should give more information at high  $p_m$ , a region which is, however, difficult to explore experimentally. These diagrammatic evaluations ultimately gave way to more refined, full Faddeev calculations performed independently by the Krakow [23,24] and the Hannover/Lisbon [25–28] groups, which we use in this paper. The key feature of our experiment is the unmatched precision of the extracted asymmetries together with a broad kinematic range, with  $p_m$  extending to as far as 250 MeV/c. This extended coverage represents a crucial advantage, since Faddeev calculations indicate that the manifestations of various wave-function components, as

well as the potential effects of three-nucleon forces, imply very different signatures as functions of  $p_m$ .

If both beam and target are fully polarized, the cross-section for the  $^3\text{He}(\vec{e}, e'p)$  reaction has the form

$$\frac{d\sigma(h, \vec{S})}{d\Omega} = \frac{d\sigma_0}{d\Omega} \left[ 1 + \vec{S} \cdot \vec{A}^0 + h(A_e + \vec{S} \cdot \vec{A}) \right],$$

where  $d\Omega = d\Omega_e dE_e d\Omega_p$  is the differential of the phase-space volume,  $\sigma_0$  is the unpolarized cross section,  $\vec{S}$  is the spin of the target, and  $h$  is the helicity of the electrons. Here  $\vec{A}^0$  and  $A_e$  are the target and beam analyzing powers, respectively, while the spin-correlation parameters  $\vec{A}$  yield the asymmetries when both the beam and the target are polarized. If the target is polarized only in the horizontal plane defined by the beam and scattered electron momenta, the term  $\vec{S} \cdot \vec{A}^0$  does not contribute [20], while  $A_e$  is suppressed and is negligible with respect to  $\vec{A}$ .

The orientation of the target polarization is defined by the angles  $\theta^*$  and  $\phi^*$  in the frame where the  $z$ -axis is along  $\vec{q}$  and the  $y$ -axis is given by  $\vec{p}_e \times \vec{p}'_e$ . The measured asymmetry at given  $\theta^*$  and  $\phi^*$  is then

$$A(\theta^*, \phi^*) = \vec{S}(\theta^*, \phi^*) \cdot \vec{A} = \frac{(\frac{d\sigma}{d\Omega})_+ - (\frac{d\sigma}{d\Omega})_-}{(\frac{d\sigma}{d\Omega})_+ + (\frac{d\sigma}{d\Omega})_-},$$

where the subscript signs represent the beam helicities. In this paper we report on the measurements of these asymmetries in  $^3\text{He}(\vec{e}, e'p)d$  and  $^3\text{He}(\vec{e}, e'p)pn$  processes. The measurements were performed during the E05-102 experiment at the Thomas Jefferson National Accelerator Facility in experimental Hall A [29], with a beam energy of 2.425 GeV in quasi-elastic kinematics at energy transfer  $\omega \approx 140$  MeV and four-momentum transfer of  $Q^2 = \vec{q}^2 - \omega^2 \approx 0.25$  (GeV/c) $^2$ .

In the experiment we utilized a continuous, longitudinally polarized electron beam with an average polarization of  $P_e = (84.3 \pm 2.0)\%$ . The beam polarization was measured periodically by a Møller polarimeter [29], and the given uncertainty is predominantly systematic. The beam currents were between 5  $\mu\text{A}$  and 11  $\mu\text{A}$ , chosen to ensure stable operation in conjunction with the polarized target system. The target was a 40 cm-long glass cell containing  $^3\text{He}$  gas at approximately 9.3 bar (0.043 g/cm $^2$ ), polarized continuously by hybrid spin-exchange optical pumping [30–33]. Two pairs of Helmholtz coils were used to maintain the in-plane target polarization direction along the beam line and perpendicular to it, as dictated by instrumental constraints. This corresponded to the angles  $67^\circ$  and  $156^\circ$  with respect to  $\vec{q}$ , allowing us to measure  $A(67^\circ, 0^\circ)$  and  $A(156^\circ, 0^\circ)$ , respectively. Electron paramagnetic and nuclear magnetic resonance [34–36] were used to monitor the target polarization,  $P_t$ , which was between 50% and 60% when corrected for dilution due to nitrogen, close to the maximum polarization of 63% achieved without beam. The dilution factor was determined by using a reference cell filled with unpolarized  $^3\text{He}$  and different amounts of  $\text{N}_2$ , and measuring the rates at different relative pressures.

The scattered electrons were detected by a High-Resolution magnetic Spectrometer (HRS) [29] positioned at  $12.5^\circ$ , while the protons were detected by the large-acceptance spectrometer Big-Bite placed at  $75^\circ$  equipped with a detector package optimized for hadron detection [37]. The reconstructed proton momenta were corrected for energy losses in all materials from the target vertex to the detector package. Further details of the experimental setup and the procedure to extract the very pure sample of electron-proton coincidence events are given in Ref. [5].

The experimental asymmetry for each orientation of the target polarization was determined as the relative difference between the number of background-subtracted coincidence events

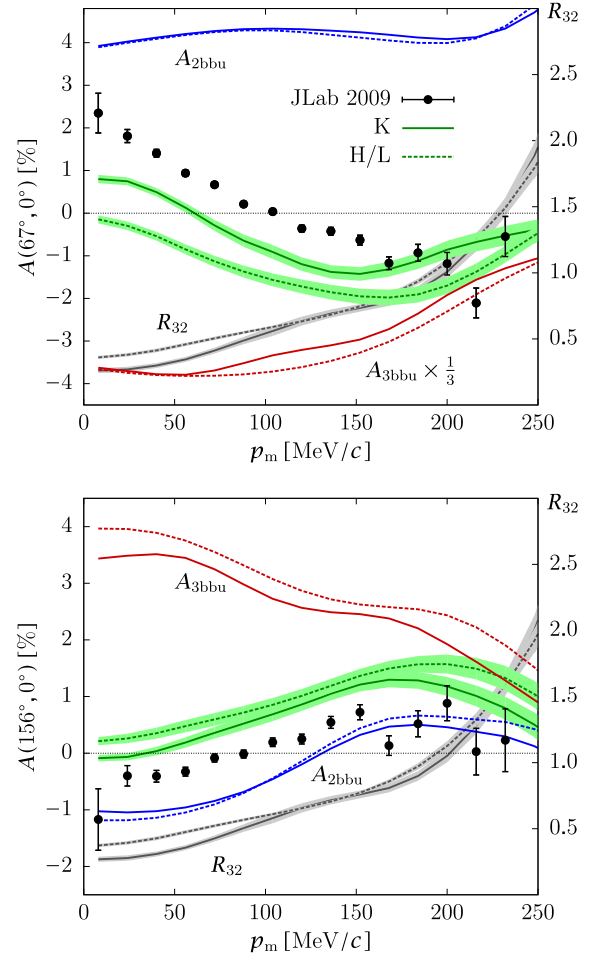


**Fig. 1.** The asymmetries  $A(67^\circ, 0^\circ)$  (top) and  $A(156^\circ, 0^\circ)$  (bottom) in the quasi-elastic  $^3\text{He}(\vec{e}, e'p)$  process (2bbu and 3bbu combined) as functions of missing momentum, compared to theoretical predictions (green) showing the 2bbu (blue) and 3bbu (red) contributions as well as the ratio of 3bbu and 2bbu cross-sections (grey, right axis). Full lines correspond to Krakow (K) calculations [23,24], while the dashed lines correspond to Hannover/Lisbon (H/L) calculations [25–28]. Only statistical uncertainties are shown. For systematical uncertainties and the meaning of the error bands see text.

corresponding to positive and negative beam helicities,  $A_{\text{exp}} = (N_+ - N_-)/(N_+ + N_-)$ , where  $N_+$  and  $N_-$  have been corrected for helicity-gated beam charge asymmetry, dead time and radiative effects. The corresponding final values of the physics asymmetries were calculated as  $A = A_{\text{exp}}/(P_e P_t)$ .

The resulting asymmetries as functions of  $p_m$  are shown in Fig. 1. The largest contribution to their systematic error comes from the relative uncertainty in the target polarization,  $P_t$ , which has been estimated at  $\pm 5\%$ , followed by the uncertainty in the target dilution factor ( $\pm 2\%$ ) and the absolute uncertainty of the beam polarization,  $P_e$  ( $\pm 2\%$ ). The background rates, determined by empty-cell measurements, were smaller than 0.3% of the total, resulting in a 0.1% systematic uncertainty of the final asymmetry. The beam-charge asymmetry was determined to be  $(-0.2 \pm 1.5) \cdot 10^{-5}$ . Other helicity-correlated false asymmetries were evaluated to be less than 0.1%, also much smaller than the measured physics asymmetry. The uncertainty in the target orientation angle represents a minor contribution ( $\pm 0.6\%$ ) to the total uncertainty, totalling  $\approx 6\%$  (relative).

Fig. 1 also shows the results of the state-of-the-art three-body Faddeev calculations of the Krakow (K) [23,24] and Hannover/Lisbon (H/L) [25–28] groups. The K calculations are based on the

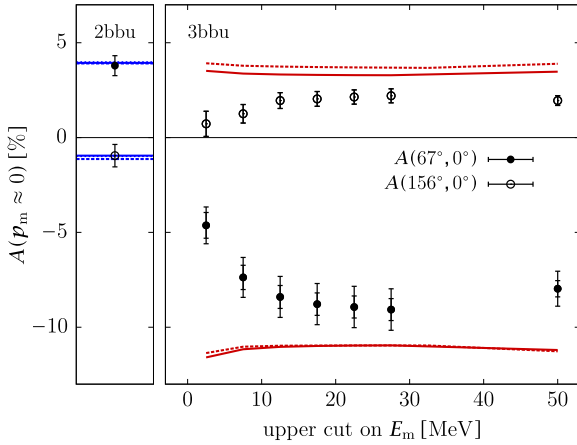


**Fig. 2.** The extracted asymmetries for 2bbu (left) and 3bbu (right). Curve notation as in Fig. 1, with the addition of the Pisa 2bbu calculation [40] in the left panel (blue dotted lines hidden beneath the full and dashed lines). See text for details.

AV18 nucleon–nucleon potential [38] and involve a complete treatment of FSI and the dominant part of MEC, but do not include three-nucleon forces; the Coulomb interaction is taken into account in the  $^3\text{He}$  bound state. The H/L calculations are based on the coupled-channel extension of the charge-dependent Bonn potential [39] and also include FSI and MEC, while the  $\Delta$  isobar is added as an active degree of freedom providing a mechanism for an effective three-nucleon force and for exchange currents. Point Coulomb interaction is added in the partial waves involving two charged baryons. In contrast to the K and H/L approaches, the Pisa (P) calculations [40] are based on a variational pair-correlated hyper-spherical harmonic expansion that is comparable in precision to the Faddeev methods and is expected to account for all relevant reaction mechanisms. The P calculations are based on the AV18 interaction model (augmented by the Urbana IX three-nucleon force [41]), in which full inclusion of FSI is taken into account, as well as MEC. At present, the Pisa group only provides 2bbu calculations. Coulomb interaction is included only in the bound state in K calculations, but in both bound and scattering states in H/L and P calculations. All these calculations reproduce sufficiently well the nuclear binding energies and charge radii [26,27,42,43]. Due to the extended experimental acceptance, all theoretical asymmetries were appropriately averaged, resulting in the error bands around the theoretical curves in Fig. 1. Details can be found in [5].

Neither the K nor the H/L calculation reproduces the measured asymmetries to a satisfactory level. Similarly to our findings in the deuteron channel, the theories approximately capture their overall functional forms, but exhibit systematic vertical offsets of up to two percent. In all calculations shown here a strong cancellation is involved in obtaining each total asymmetry from its 2bbu and 3bbu contributions, which are typically opposite in sign and of different magnitudes. Nevertheless, the failure of the theories to reproduce the data can be traced to the 3bbu asymmetry alone, as discussed in the following.

Since the energy resolution of our measurement (about 11 MeV FWHM) was insufficient to directly disentangle the 2bbu and 3bbu channels, the individual asymmetries were extracted by restricting the data sample to  $p_m \leq 60 \text{ MeV}/c$  and studying the dependence of  $A(67^\circ, 0^\circ)$  and  $A(156^\circ, 0^\circ)$  in terms of the upper cut in missing energy,  $E_m = \omega - T_p - 7.7 \text{ MeV}$ . The comparison of the measured  $E_m$  spectrum (extending below  $E_m = 0$  due to resolution effects) with the simulated one revealed that in spite of the overlap between the two channels, the lowest portion of the distribution at

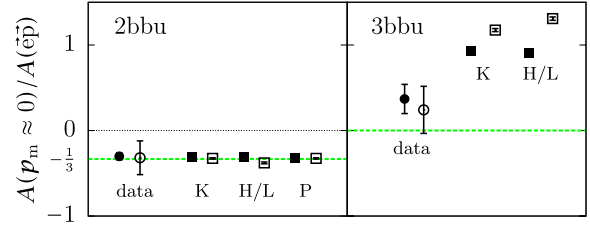


**Fig. 3.** The  $A(67^\circ, 0^\circ)$  (full symbols) and  $A(156^\circ, 0^\circ)$  (empty symbols) asymmetries for 2bbu (left) and 3bbu (right) divided by the corresponding asymmetries for elastic  $\bar{e}p$  scattering at the same value of  $Q^2$  and for  $E_m \leq 2.5 \text{ MeV}$ . In both panels the data (circles) are compared to the calculations (squares). The tiny uncertainties on the theoretical points are due to the averaging procedure.

$E_m \leq 0$  is dominated by 2bbu. There the 3bbu contributes only 7% to the total cross section, thus offering a possibility to extract the 2bbu asymmetry. The extracted asymmetry  $A_{2\text{bbu}}$  agrees well with the calculations (see Fig. 2 (left)). At the same time, a very small residual difference between the experimental result and theory (0.5% in all cases) suggests that near the threshold the size of the 3bbu asymmetry is about 1%, much smaller than the predictions. To study the 3bbu asymmetry above the threshold, the data at  $E_m > 0$  were incrementally added to the analysis. Considering that the measured asymmetries contain also the 2bbu contribution, the 3bbu asymmetry (Fig. 2 (right)) has been extracted from the data as

$$A_{3\text{bbu}} = \frac{(1 + R'_{32})A_{\text{exp}} - A_{2\text{bbu}}}{R'_{32}}.$$

Here  $R'_{32}$  is the 3bbu/2bbu cross-section ratio obtained from the  $R_{32}$  shown in Fig. 1 by considering  $E_m$  up to a specific maximum value, with  $p_m \approx 0$ , and correcting for finite momentum and angular resolutions as well as radiative effects. Typically  $R'_{32}$  ranges from 0.20 to 0.33 and is assumed to be well under control in both K and H/L calculations, with an uncertainty of about 10%. The extracted asymmetries are in good agreement with the theory in the limit where the whole spectrum ( $E_m \leq 50 \text{ MeV}$ ) is considered in the analysis, but strongly deviate from the theory near threshold ( $E_m \leq 2.5 \text{ MeV}$ ) for the 3bbu reaction channel.

In an effort to compensate for the effect of spin orientation of protons inside the polarized  $^3\text{He}$  nucleus, we have divided the nuclear asymmetries by the asymmetries for elastic  $\bar{e}p$  scattering [44] at the same value of four-momentum transfer; see Fig. 3. In a simplified picture of the  $^3\text{He}(\bar{e}, e'p)$  process, one would expect the 2bbu ratio at  $p_m \approx 0$  to be  $-1/3$ , corresponding to the effective polarization of the (almost free) proton inside the polarized  $^3\text{He}$  nucleus, while the 3bbu ratio should vanish because either of the two oppositely polarized protons could be knocked out in the process. Indeed, in the 2bbu case both the experimental and the predicted ratios coincide almost perfectly, at the anticipated “naive” value of  $-1/3$ . On the other hand, in the 3bbu case the predictions cluster approximately around unity (and apparently retain a residual dependence on  $\theta^*$ ), while the two experimental ratios are much smaller (and mutually consistent).

In conclusion, we have provided the world-first, high-precision measurement of double-polarization asymmetries for proton knockout from polarized  $^3\text{He}$  nuclei at two different spin settings and over a broad range of momenta. Two state-of-the-art theoretical approaches to the  $^3\text{He}$  disintegration process are able to approximately accommodate the main structural features of our data set. Since the asymmetries are rather small and strong cancellations of the two-body and three-body breakup contributions are involved, the agreement can be deemed satisfactory and the theoretical framework justified. However, the high precision of our



measurements has been able to reveal a substantial deficiency in the calculations of the three-body breakup process, presumably due to a mismatch between the true relativistic kinematics and non-relativistic spin-dependent nuclear dynamics employed in the calculations.

On the other hand, since the three-body breakup process is more selective than the corresponding two-body breakup of  $^3\text{He}$ , it will be interesting to investigate if an application of consistent chiral two-nucleon and three-nucleon interactions with chiral two-nucleon and three-nucleon contributions in the electromagnetic current operator could also shed light on this problem.

## Acknowledgements

We thank the Jefferson Lab Hall A and Accelerator Operations technical staff for their outstanding support. This work was supported in part by the National Science Foundation and the U.S. Department of Energy. Jefferson Science Associates, LLC, operates Jefferson Lab for the U.S. DOE under U.S. DOE contract DE-AC05-06OR23177. This work was supported in part by the Slovenian Research Agency (research core funding No. P1-0102). This work is a part of the LENPIC project and was supported by the Polish National Science Centre under Grants No. 2016/22/M/ST2/00173 and 2016/21/D/ST2/01120. The numerical calculations of the Krakow group were partially performed on the supercomputer cluster of the JSC, Jülich, Germany.

## References

- [1] W. Glöckle, et al., *Eur. Phys. J. A* 21 (2004) 335.
- [2] J. Golak, et al., *Phys. Rep.* 415 (2005) 89.
- [3] M.O. Distler, *Few-Body Syst.* 43 (2008) 51.
- [4] S. Širca, *Few-Body Syst.* 47 (2010) 39.
- [5] M. Mihovilović, et al., *Phys. Rev. Lett.* 113 (2014) 232505.
- [6] R.E.J. Florizone, et al., *Phys. Rev. Lett.* 83 (1999) 2308.
- [7] A. Kozlov, et al., *Phys. Rev. Lett.* 93 (2004) 132301.
- [8] M.M. Rvachev, *Phys. Rev. Lett.* 94 (2005) 192302.
- [9] F. Benmokhtar, *Phys. Rev. Lett.* 94 (2005) 082305.
- [10] H. Baghdasaryan, et al., *Phys. Rev. C* 85 (2012) 064318.
- [11] W.P. Ford, R. Schiavilla, J.W.V. Orden, *Phys. Rev. C* 89 (2014) 034004.
- [12] M. Alvioli, C.C. degli Atti, L.P. Kaptari, *Phys. Rev. C* 81 (2010) 021001.
- [13] C.C. degli Atti, L.P. Kaptari, *Phys. Rev. Lett.* 95 (2005) 052502.
- [14] C.C. degli Atti, L.P. Kaptari, *Phys. Rev. Lett.* 100 (2008) 122301.
- [15] R. Schiavilla, O. Benhar, A. Kievsky, L.E. Marcucci, M. Viviani, *Phys. Rev. C* 72 (2005) 064003.
- [16] H.R. Poolman, et al., *Phys. Rev. Lett.* 84 (2000) 3855.
- [17] D.W. Higinbotham, et al., *Nucl. Instrum. Methods A* 444 (2000) 557.
- [18] C. Carasco, et al., *Phys. Lett. B* 559 (2003) 41.
- [19] P. Achenbach, et al., *Eur. Phys. J. A* 25 (2005) 177.
- [20] J.-M. Laget, *Phys. Lett. B* 276 (1992) 398.
- [21] S. Nagorny, W. Turchinets, *Phys. Lett. B* 389 (1996) 429.
- [22] S. Nagorny, W. Turchinets, *Phys. Lett. B* 429 (1998) 222.
- [23] J. Golak, et al., *Phys. Rev. C* 65 (2002) 064004.
- [24] J. Golak, et al., *Phys. Rev. C* 72 (2005) 054005.
- [25] L.P. Yuan, K. Chmielewski, M. Oelsner, P.U. Sauer, J. Adam, *Phys. Rev. C* 66 (2002) 054004.
- [26] A. Deltuva, L.P. Yuan, J. Adam, A.C. Fonseca, P.U. Sauer, *Phys. Rev. C* 69 (2004) 034004.
- [27] A. Deltuva, L.P. Yuan, J. Adam, P.U. Sauer, *Phys. Rev. C* 70 (2004) 034004.
- [28] A. Deltuva, A.C. Fonseca, P.U. Sauer, *Phys. Rev. C* 71 (2005) 054005.
- [29] J. Alcorn, et al., *Nucl. Instrum. Methods A* 522 (2004) 294.
- [30] T.G. Walker, W. Happer, *Rev. Mod. Phys.* 69 (1997) 629.
- [31] S. Appelt, et al., *Phys. Rev. A* 58 (1998) 1412.
- [32] E. Babcock, I.A. Nelson, S. Kadlecik, B. Driehuys, L.W. Anderson, F.W. Hersman, T.G. Walker, *Phys. Rev. Lett.* 91 (2003) 123003.
- [33] J.T. Singh, P.A.M. Dolph, W.A. Tobias, T.D. Averett, A. Kelleher, K.E. Mooney, V.V. Nelyubin, Y. Wang, Y. Zheng, G.D. Cates, *Phys. Rev. C* 91 (2015) 055205.
- [34] A. Abragam, *Principles of Nuclear Magnetism*, Oxford University Press, 1961.
- [35] M.V. Romalis, G.D. Cates, *Phys. Rev. A* 58 (1998) 3004.
- [36] E. Babcock, I.A. Nelson, S. Kadlecik, T.G. Walker, *Phys. Rev. A* 71 (2005) 013414.
- [37] M. Mihovilović, et al., *Nucl. Instrum. Methods A* 686 (2012) 20.
- [38] R.B. Wiringa, V.G.J. Stoks, R. Schiavilla, *Phys. Rev. C* 51 (1995) 38.
- [39] R. Machleidt, *Phys. Rev. C* 63 (2001) 024001.
- [40] L.E. Marcucci, M. Viviani, R. Schiavilla, A. Kievsky, S. Rosati, *Phys. Rev. C* 72 (2005) 014001.
- [41] B.S. Pudliner, V.R. Pandharipande, J. Carlson, R.B. Wiringa, *Phys. Rev. Lett.* 74 (1995) 4396.
- [42] A. Nogga, A. Kievsky, H. Kamada, W. Glöckle, L.E. Marcucci, S. Rosati, M. Viviani, *Phys. Rev. C* 67 (2003) 034004.
- [43] A. Kievsky, S. Rosati, M. Viviani, L.E. Marcucci, L. Girlanda, J. Phys. G, *Nucl. Part. Phys.* 35 (2008) 063101.
- [44] H. Gao, *Int. J. Mod. Phys. E* 12 (2003) 1.